Proceedings of the ASME 2010 4th International Conference on Energy Sustainability
ES2010
May 17-22, 2010, Phoenix, Arizona, USA

ES2010-90192

RADIATIVE COOLING IN NORTHERN EUROPE USING A ROOF WINDOW

Martin Fält
Thermal and Flow Engineering
Åbo Akademi University
Turku, Finland
martin.falt@abo.fi

Ron Zevenhoven ASME member
Thermal and Flow Engineering
Åbo Akademi University
Turku, Finland
ron.zevenhoven@abo.fi

ABSTRACT

The design and performance of a triple glass window used as a roof component was analyzed in this paper. A mathematical model was set up for the component and weather data for the Finnish city Helsinki was used to assess its performance. This roof component would act as a passive radiative cooler during the summer and as a thermal insulator during the rest of the year. This versatile usage of the window component would thus decrease the need for traditional air-conditioning during summer and hence save electricity. The triple glass window would consist of one normal silica window and of two High Density Polyethylene (HPDE) windows. The space between the three windows would contain a (pressurized) greenhouse gas that would act as the heat carrier in this system. The heat would be transferred in to the system to the gas by heat radiation, conduction and natural convection through the window facing the room. This heated gas would then rise to the upper vacant space due to a decrease in the gases density caused by the heating. In the upper vacant part, the gas would then be cooled by radiative cooling through the HDPE, and the atmospheric window with colder air masses in the upper atmosphere. When, the greenhouse gas would have cooled down its density would increase and the gas would drop to the lower part of the window component. During times when no cooling would be needed the connection between the two vacant spaces would be cut, thus changing the roof components' task from a passive radiative cooler to a thermal insulator. The heating of the space due to sunshine is of course evident and lower temperatures would be achieved if no window at all be used, but for places were roof windows are built this component would offer a viable alternative. This paper is a continuation to the paper by Zevenhoven and Fält submitted to this conference **(1)**.

INTRODUCTION

Radiative cooling is a passive cooling method that connects a warm object on a building to a lower sky temperature; one could describe it as an inverse solar collector. Investigations have been made if flat-plate solar collectors could be used for radiative cooling (2). Radiative cooling is a method that uses less energy than contemporary cooling devices that use the vapor compression cycle. Radiative cooling works best during the night when it is not cancelled out by the incoming heat radiation from the sun (3). However, studies have also been made if this cooling system could be used during the day by the use of reflecting polyethylene films (4). The problem with radiative cooling is that the effect per unit area is low and therefore large radiators have to be acquired which make them expensive.

This article will evaluate a system that combines radiative cooling with a roof window. Even though roof windows heat the room that is below it, they are used widely. The main reason for using roof window is that it brings light into a space, but simultaneously it also brings heat in the form of light. This heat can often be unwanted and therefore has to be removed. This article will also evaluate how the window would perform during the winter when no cooling is needed, that is as insulation. To work as both a cooling device and as insulation, the roof window has to be adjustable according to seasonal variations. A schematic view of the roof window can be seen in Figure 1 and Figure 2. It is noted that only long-wave thermal radiation is considered in this article, excluding thermal radiation at shorter wavelengths from the sun.

NOMENCLATURE

A	Area [m^2]
C	Coefficient of discharge, between 0.6 and 1 [-]
c_p	Mass specific heat at constant pressure []
d	Thickness of a material [m]
DIA	Diamter of the window [m]
E_b	Blackbody of a material [W/m^2]
F	View factor for radiation calculations [-]
g	Gravity constant [m/s^2]
Gr	Grashof number
HPDE	High Density Polyethylene
h	Convective heat transfer

Copyright © 2010 by ASME

H Height or thickness of window three [m]
H_s Height of site were the roof window is installed [m]
H_w Height of wind tower [m]
J_{room} Blackbody corresponding to the node that the room exchanges radiative heat with [W/m^2]
J_{sky} Blackbody corresponding to the node that the sky exchanges radiative heat with [W/m^2]
k Conductivity of a material [W/ (K m^2)]
L Length of the window [m]
MR Modulus of rupture, [MPa]
Nu Nusselt number [-]
p Pressure, [MPa]
P Pressure differential [MPa]
Pr Prandtl number [-]
$\dot{Q}_{long\ wave}$ Heat flow of long wave heat radiation [W/m^2]
R Resistance to heat transfer [-]
S_b Blackbody of a surface between two layers of different material [W/m^2]
T Temperature [K]
T_∞ Temperature of the room [K]
T_w Temperature of the window [K]
Th Thickness of window [m]
v Wind speed at measured site [m/s]

Greek letters
α_w Alpha terrain parameter for weather tower [-]
α_s Alpha terrain parameter for the site where the roof window is installed [-]
β Coefficient of thermal expansion [1/K]
γ, w Gamma terrain parameter for weather tower [-]
ε Emissivity of a material [-]
ε, ξ Constants for the determination of Nu, are assumed to be equal to zero in this case [-]
μ Viscosity [Pa s]
ρ Density [kg^3/m^3]
σ Stefan Boltzman constant 5.67×10^{-8} W/ (K m^2)
τ Transmissivity of a material [-]

Subscripts
$g1$ Gas one
$g2$ Gas two
$gl1$ Glass one
$gl2$ Glass two
$gl3$ Glass three
$1-21, A, B$ Radiative resistances
$I-XV, C, D$ Conductive and convective resistances

SYSTEM DESCRIPTION

Since the system can be controlled accordingly to if cooling is needed or not two different modes have to exist. The first mode, the cooling mode, is pictured in Figure 1 and the second mode, the insulating mode, is pictured in Figure 2.

This system consists of a triple glass window where the two outer glasses are made of HDPE and the glass in the middle is made of normal silica glass. The spaces between these three windows contain a (pressurized) greenhouse gas that acts as a heat carrier in the system. In this article, the greenhouse gas consists of pure CO_2, but other greenhouse gases can also be taken into consideration. Heat is transferred in to the system, to the gas, by radiation, conduction and natural convection through the window facing the room below. This heated gas then rises to the upper vacant space due to a decrease in the gases density caused by the heating. In the upper vacant part, the gas is then cooled by radiative cooling through the HDPE, and the atmospheric window with colder air masses in the upper atmosphere. Then when the greenhouse gas cools down its density increases and it drops down to the lower part of the window system. During times when no cooling is needed the connection between the two gas spaces is cut, thus changing the roof components' task from a passive radiative cooler to a thermal insulator.

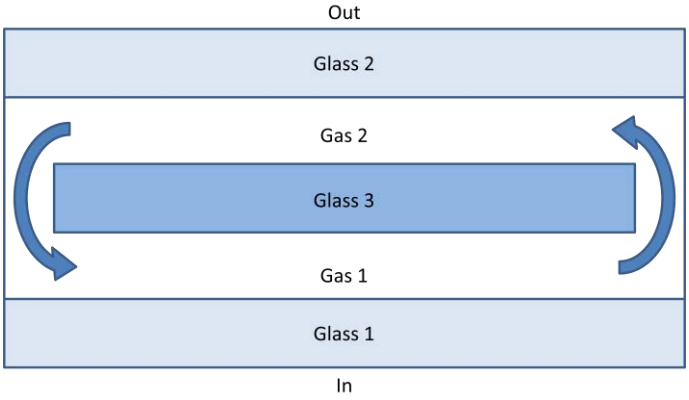

Figure 1 Roof window in cooling mode

Figure 2 Roof window in insulating mode

THEORETICAL ANALYSIS

Since transfer of heat radiation, convection and conduction are all taken into account a system that combines these different heat transfer methods has to be established. The system that is used here is called the "additive solution" where the radiation transfer is solved separately from the convection and conduction part and then combined. The additive method is reported having accuracy of 10% for calculating heat flows for black plates (5). However, the method is reported having problems predicting temperatures, which originates from the fact that the temperature in the case of the conduction and

Copyright © 2010 by ASME

convection only affects the heat flow in the power of the first while it does this in the power of the fourth for the radiation part. However, since temperature differences are relatively small in our case the additive method is also used to calculate the temperatures. This is done by first calculating the temperatures of the gas separately for the radiative case and for the convective and conductive case, after which a weighted mean of the temperature is calculated which is dependent of the magnitude of the heat flow.

To solve this heat transfer problem, heat transfer networks were set-up to illustrate how the different heat transfer takes place. Networks were separately set-up for the radiation case and for the conduction and convection case. The radiation network is shown in Figure 3.

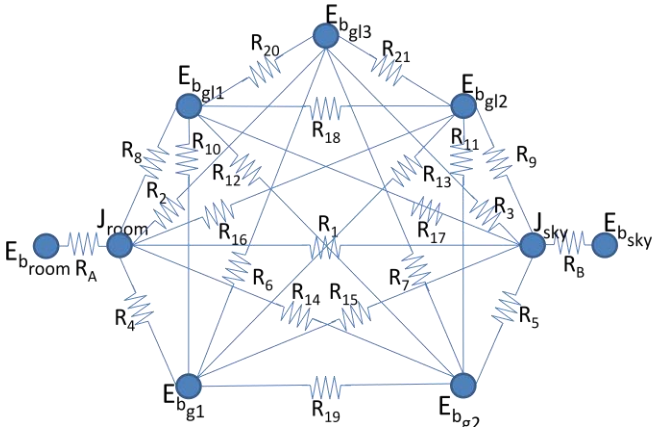

Figure 3 Resistance network for radiative heat transfer

This resistance network shows the heat transfer between the sky and the room through the glasses and gases. The resistances in Figure 3 are given by the Equations 1 to 23.

Table 1 Resistances to radiative heat transfer

Describes the resistance to radiative heat transfer directly from J_1 to J_2	$R_1 = \frac{1}{A\,F\tau_{gl1}\tau_{g1}\tau_{gl3}\tau_{g2}\tau_{gl2}}$	(1)
Describes the resistance to radiative heat transfer directly from J_1 to $E_{b_{gl2}}$	$R_2 = \frac{1}{A\,F\tau_{gl1}\tau_{g1}\varepsilon_{gl3}}$	(2)
Describes the resistance to radiative heat transfer directly from J_2 to $E_{b_{gl2}}$	$R_3 = \frac{1}{A\,F\tau_{gl2}\tau_{g2}\varepsilon_{gl3}}$	(3)
Describes the resistance to radiative heat transfer directly from J_1 to $E_{b_{gl3}}$	$R_4 = \frac{1}{A\,F\tau_{gl1}\varepsilon_{g1}}$	(4)
Describes the resistance to radiative heat transfer directly from J_2 to $E_{b_{g2}}$	$R_5 = \frac{1}{A\,F\tau_{gl2}\varepsilon_{g2}}$	(5)
Describes the resistance to radiative heat transfer directly from $E_{b_{gl3}}$ to $E_{b_{gl2}}$	$R_6 = \frac{1}{A\,F\varepsilon_{g1}\varepsilon_{gl3}}$	(6)
Describes the resistance to radiative heat transfer directly from $E_{b_{g2}}$ to $E_{b_{gl2}}$	$R_7 = \frac{1}{A\,F\varepsilon_{g2}\varepsilon_{gl3}}$	(7)
Describes the resistance to radiative heat transfer directly from J_1 to $E_{b_{gl1}}$	$R_8 = \frac{1}{A\,F\varepsilon_{gl1}}$	(8)
Describes the resistance to radiative heat transfer directly from J_2 to $E_{b_{g1}}$	$R_9 = \frac{1}{A\,F\varepsilon_{gl2}}$	(9)
Describes the resistance to radiative heat transfer directly from $E_{b_{gl1}}$ to $E_{b_{gl3}}$	$R_{10} = \frac{1}{A\,F\varepsilon_{gl1}\varepsilon_{g1}}$	(10)
Describes the resistance to radiative heat transfer directly from $E_{b_{g1}}$ to $E_{b_{g2}}$	$R_{11} = \frac{1}{A\,F\varepsilon_{gl2}\varepsilon_{g2}}$	(11)
Describes the resistance to radiative heat transfer directly from $E_{b_{gl1}}$ to $E_{b_{g2}}$	$R_{12} = \frac{1}{A\,F\varepsilon_{gl1}\tau_{g1}\tau_{gl3}\varepsilon_{g2}}$	(12)
Describes the resistance to radiative heat transfer directly from $E_{b_{g1}}$ to $E_{b_{gl3}}$	$R_{13} = \frac{1}{A\,F\varepsilon_{gl2}\tau_{g2}\tau_{gl3}\varepsilon_{g1}}$	(13)
Describes the resistance to radiative heat transfer directly from J_1 to $E_{b_{g2}}$	$R_{14} = \frac{1}{A\,F\tau_{gl1}\tau_{g1}\tau_{gl3}\varepsilon_{g2}}$	(14)
Describes the resistance to radiative heat transfer directly from J_2 to $E_{b_{gl3}}$	$R_{15} = \frac{1}{A\,F\tau_{gl2}\tau_{g2}\tau_{gl3}\varepsilon_{g1}}$	(15)
Describes the resistance to radiative heat transfer directly from J_1 to $E_{b_{g1}}$	$R_{16} = \frac{1}{A\,F\tau_{gl1}\tau_{g1}\tau_{gl3}\tau_{g2}\varepsilon_{gl2}}$	(16)
Describes the resistance to radiative heat transfer directly from J_2 to $E_{b_{gl1}}$	$R_{17} = \frac{1}{A\,F\tau_{gl2}\tau_{g2}\tau_{gl3}\tau_{g1}\varepsilon_{gl1}}$	(17)
Describes the resistance to radiative heat transfer directly from $E_{b_{gl1}}$ to $E_{b_{g1}}$	$R_{18} = \frac{1}{A\,F\varepsilon_{gl1}\tau_{g1}\tau_{gl3}\tau_{g2}\varepsilon_{gl2}}$	18)
Describes the resistance to radiative heat transfer directly from $E_{b_{gl3}}$ to $E_{b_{g2}}$	$R_{19} = \frac{1}{A\,F\varepsilon_{g1}\tau_{gl3}\varepsilon_{g2}}$	(19)
Describes the resistance to radiative heat transfer directly from $E_{b_{gl1}}$ to $E_{b_{gl2}}$	$R_{20} = \frac{1}{A\,F\varepsilon_{gl1}\tau_{g1}\varepsilon_{gl3}}$	(20)
Describes the resistance to radiative heat transfer directly from $E_{b_{g1}}$ to $E_{b_{gl2}}$	$R_{21} = \frac{1}{A\,F\varepsilon_{gl2}\tau_{g2}\varepsilon_{gl3}}$	(21)
Describes the resistance to radiative heat transfer by the room	$R_A = \frac{1-\varepsilon_1}{A_1\,\varepsilon_1}$	(22)
Describes the resistance to radiative heat transfer by the sky	$R_B = \frac{1-\varepsilon_2}{A_2\,\varepsilon_2}$	(23)

Figure 3 illustrates also that an energy balance can be set-up for each point in the heat transfer network. This results in

Copyright © 2010 by ASME

a set of equations consisting of Equations 24-30. The energy balance for J_{room} describes the radiative heat transfer of the blackbody corresponding to that which the room exchanges radiative heat with:

$$\frac{J_{room}-J_{sky}}{R_1}+\frac{J_{room}-E_{b_{gl1}}}{R_8}+\frac{J_{room}-E_{b_{g1}}}{R_{16}}+\frac{J_{room}-E_{b_{gl3}}}{R_4}+\frac{J_{room}-E_{b_{g2}}}{R_{14}}+\frac{J_{room}-E_{b_{gl2}}}{R_2}=\frac{J_{room}-E_A}{R_A} \quad (24)$$

Energy balance for J_{sky} describes the radiative heat transfer of the blackbody corresponding to that which the sky exchanges radiative heat with:

$$\frac{J_{sky}-J_{room}}{R_1}+\frac{J_{sky}-E_{b_{gl1}}}{R_{17}}+\frac{J_{sky}-E_{b_{g1}}}{R_9}+\frac{J_{sky}-E_{b_{gl3}}}{R_{15}}+\frac{J_{sky}-E_{b_{g2}}}{R_5}+\frac{J_{sky}-E_{b_{gl2}}}{R_4}=\frac{J_{sky}-E_B}{R_B} \quad (25)$$

Energy balance for $E_{b_{gl1}}$ describes the radiative heat transfer of the blackbody corresponding to glass 1:

$$\frac{E_{b_{gl1}}-J_{room}}{R_8}+\frac{E_{b_{gl1}}-J_{sky}}{R_{17}}+\frac{E_{b_{gl1}}-E_{bg1}}{R_{18}}+\frac{E_{b_{gl1}}-E_{b_{gl3}}}{R_{10}}+\frac{E_{b_{gl1}}-E_{b_{g2}}}{R_{12}}+\frac{E_{b_{gl1}}-E_{b_{gl2}}}{R_{20}}=0 \quad (26)$$

Energy balance for $E_{b_{g1}}$ describes the radiative heat transfer of the blackbody corresponding to gas layer 1:

$$\frac{E_{b_{g1}}-J_{room}}{R_{16}}+\frac{E_{b_{g1}}-J_{sky}}{R_9}+\frac{E_{b_{g1}}-E_{b_{gl1}}}{R_{18}}+\frac{E_{b_{g1}}-E_{b_{gl3}}}{R_{13}}+\frac{E_{b_{g1}}-E_{b_{g2}}}{R_{11}}+\frac{E_{b_{g1}}-E_{b_{gl2}}}{R_{21}}=0 \quad (27)$$

Energy balance for $E_{b_{gl3}}$ describes the radiative heat transfer of the blackbody corresponding to glass 3:

$$\frac{E_{b_{gl3}}-J_{room}}{R_4}+\frac{E_{b_{gl3}}-J_{sky}}{R_{15}}+\frac{E_{b_{gl3}}-E_{b_{gl1}}}{R_{10}}+\frac{E_{b_{gl3}}-E_{b_{g1}}}{R_{13}}+\frac{E_{b_{gl3}}-E_{b_{g2}}}{R_{19}}+\frac{E_{b_{gl3}}-E_{b_{gl2}}}{R_6}=0 \quad (28)$$

Energy balance for $E_{b_{g2}}$ describes the radiative heat transfer of the blackbody corresponding to gas layer 2:

$$\frac{E_{b_{g2}}-J_{room}}{R_{14}}+\frac{E_{b_{g2}}-J_{sky}}{R_5}+\frac{E_{b_{g2}}-E_{b_{gl1}}}{R_{12}}+\frac{E_{b_{g2}}-E_{b_{g1}}}{R_{11}}+\frac{E_{b_{g2}}-E_{b_{gl3}}}{R_{19}}+\frac{E_{b_{g2}}-E_{b_{gl2}}}{R_7}=0 \quad (29)$$

Energy balance for $E_{b_{gl2}}$ describes the radiative heat transfer of the blackbody corresponding to glass 2:

$$\frac{E_{b_{gl2}}-J_{room}}{R_2}+\frac{E_{b_{gl2}}-J_{sky}}{R_3}+\frac{E_{b_{gl2}}-E_{b_{gl1}}}{R_{20}}+\frac{E_{b_{gl2}}-E_{b_{g1}}}{R_{21}}+\frac{E_{b_{gl2}}-E_{b_{gl3}}}{R_6}+\frac{E_{b_{gl2}}-E_{b_{g2}}}{R_7}=0 \quad (30)$$

The emissivity of the gas in layers 1 and 2 is one of the variables that affect the overall performance of the system. The emissivity of the gas is dependent of the temperature, pressure and of the length of the gas layer; of these, the two latest can be adjusted. The emissivity of the gas is calculated according to that described in the Annex A. The pressure of the gas affects not only the emissivity of the gas but also the thickness of the glass. Therefore, a way to calculate the needed thickness of the glass is needed; this is given by Equation 31.

$$Th=\sqrt{\frac{1.1\times P\times DIA^2}{MR}} \quad (31)$$

The variation of the glass thickness in turn affects its´ transmissivity. For correcting the transmissivity of the glass, Equation 32 is used (6).

$$\tau_{real}=\tau_{measured}^{\ \frac{d_{real}}{d_{measured}}} \quad (32)$$

Since the two different modes of the roof window differentiate from each other in the way they transfer conductive and convective heat, two separate resistance networks are set up. The heat network that describes the cooling mode is pictured in Figure 4 and that for the insulating mode in Figure 5.

Copyright © 2010 by ASME

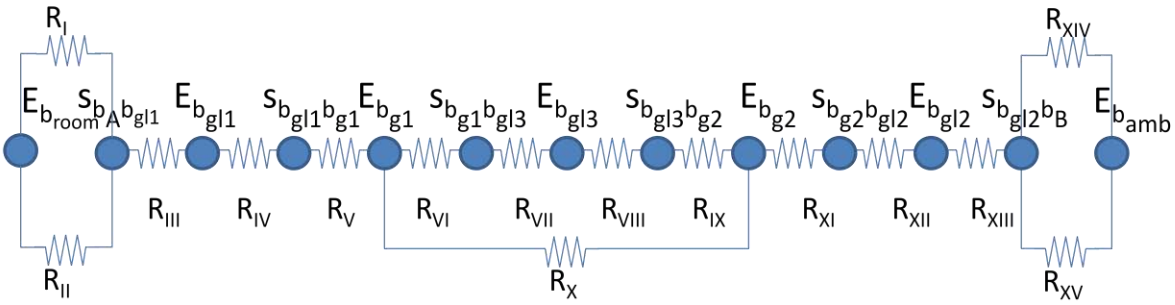

Figure 4 Resistance network for conductive & convective heat transfer for the cooling mode

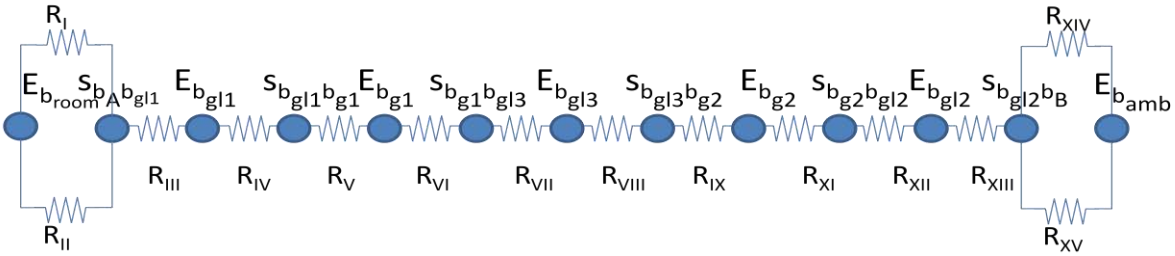

Figure 5 Resistance network for conductive & convective heat transfer for the insulating mode

The resistances that are shown in Figure 4 and Figure 5 are given in Table 2.

Table 2 Resistances to conductive and convective heat transfer

Describes the resistance to conductive heat transfer in the air from the room to the surface of the glass facing the room	$R_I = \frac{d_{room}}{k_{air}}$	(33)
Describes the resistance to convective heat transfer in the room due to the temperature difference of the window facing the room	$R_{II} = \frac{1}{h_{room}\, A}$	(34)
Describes the resistance to conductive heat transfer in the window material to the windows middle point	$R_{III} = \frac{d_{gl1}}{2k_{gl1}}$	(35)
Describes the resistance to conductive heat transfer in the window material from the middle point to its' surface	$R_{IV} = \frac{d_{gl1}}{2k_{gl1}}$	(36)
Describes the resistance to conductive heat transfer in the gas from the surface of window one to the middle point of gas one	$R_V = \frac{L_{g1}}{2k_{g1}}$	(37)
Describes the resistance to conductive heat transfer in the gas from the middle point of the gas to the surface facing the room of window three	$R_{VI} = \frac{L_{g1}}{2k_{g1}}$	(38)
Describes the resistance to conductive heat transfer in the material of window three from its' surface facing the room to its' middle point	$R_{VII} = \frac{d_{gl3}}{2k_{gl3}}$	(39)
Describes the resistance to conductive heat transfer in gas from the surface of window three, facing the sky, to the middle point of the second gas layer	$R_{VIII} = \frac{d_{gl3}}{2k_{gl3}}$	(40)
Describes the resistance to conductive heat transfer in gas from the middle point of the second layer of gas to the surface of window two facing the room	$R_{IX} = \frac{L_{g2}}{2k_{g2}}$	(41)
Describes the resistance to convective heat transfer induced by the density differences between the two gas layers	$R_X = \frac{1}{h_{grav}\, A}$	(42)
Describes the resistance to conductive heat transfer in the gas from the middle point of the second gas layer to the surface of window two facing the room	$R_{XI} = \frac{L_{g2}}{2k_{g2}}$	(43)
Describes the resistance to conductive heat transfer in the material of window two from the surface of window two facing the room to the middle of window two	$R_{XII} = \frac{d_{gl2}}{2k_{gl2}}$	(44)
Describes the resistance to conductive heat transfer in the material in the material of window two from the middle point of window two to the surface of window two facing the sky	$R_{XIII} = \frac{d_{gl2}}{2k_{gl2}}$	(45)

Copyright © 2010 by ASME

Describes the resistance to conductive heat transfer in the air from the surface of window two to the surroundings	$R_{XIV} = \frac{d_{sur}}{k_{air}}$	(46)
Describes the resistance to convective heat transfer in the air due to the wind from the surface of window two to the surroundings	$R_{XV} = \frac{1}{h_{wind}\, A}$	(47)

The wind that blows parallel to the roof window causes heat transfer by forced convection. To calculate this forced convection Equations 48 and 49 are used. These equations give the convective heat transfer for turbulent heat flows over smooth surfaces at low wind speeds (<3 m/s). The wind speed used in Equation 48 is a reduced wind speed that takes into account that the wind speed measured is different from that flowing across the window (7).

$$h_{wind} = 1.8 + 3.8v^{'}\left[\frac{W}{m^2\text{°C}}\right] \quad (48)$$

For our case the wind data that was acquired, was measured at a height of 10m and the assumed roof window is set at a height of 5m. From this, a correction of the wind speed is made using Equation 49.

$$v^{'} = \frac{\alpha_w \left({H_w}/{10}\right)^{\gamma,w}}{\alpha_s \left({H_s}/{10}\right)^{\gamma,s}} \times v \quad (49)$$

Since the glass, facing the room has a lower temperature than the room; heat transfer by natural convection will take place. The extent of this heat transfer can be calculated with Equations 50 and 51. This is a simplified equation for heat transfer by natural convection for laminar flow (8).

$$h_{room} = 1.32\sqrt[4]{\frac{\Delta T}{L}} \quad (50)$$

$$\Delta T = T_{gl1} - T_{room} \quad (51)$$

When, the roof window is set in its' cooling mode the heat transfer between the two gas layers can be calculated by Equations 52 through 54. These equations describe the heat transfer between two adjoining rooms, which is separated by a height of *H* that is driven by the temperature difference between the two gas layers (9).

$$Nu = \frac{hH}{\lambda} = \frac{C}{3}\left(\frac{g\Delta\rho H_a^3}{{\mu^2}/{\rho}}\right)^{1/2+\varepsilon}\left(\frac{c_p\mu}{\lambda}\right)^{1-\xi} = \quad (52)$$

$$\frac{C}{3}\left(\frac{g\rho^2\beta\Delta T H_a^3}{\mu^2}\right)^{1/2+\varepsilon}\left(\frac{c_p\mu}{\lambda}\right)^{1-\xi} = \frac{C}{3}Gr^{1/2+\varepsilon}\cdot Pr^{1+\xi}$$

Where:

$$\beta = \frac{1}{\overline{T}}, \Delta T = T_{g1} - T_{g2} \quad (53)$$

and

$$\frac{\Delta\rho}{\bar{\rho}} = \frac{\Delta T}{\overline{T}}; \overline{T} = \frac{T_{g1} + T_{g2}}{2};\ \bar{\rho}\frac{\rho_{g1} + \rho_{g2}}{2} \quad (54)$$

Matlab R2007B was used for all the calculations, simulations, modeling, and graphics given below.

MODELING

For the analysis of the model and for simulations purposes, weather data was acquired for a location in Helsinki, Finland (60° 10′ 15″ N, 24° 56′ 15″ E) from the Finnish meteorological institute. The data contains the hourly data of the ambient temperature, wind speed, long and short wave heat radiation data. From the long-wave radiation data, the temperature of T_{sky} could be calculated with Equation 55. Since T_{sky} is calculated as it was a blackbody, that is, it´s emissivity is equal to one, the need for speculating the emissivity of the sky becomes unnecessary in the model and in the simulations.

$$T_{sky} = \sqrt[4]{\frac{\dot{Q}_{long\ wave}}{\sigma}} \quad (55)$$

To analyze the model, some weather data constants needed to be determined; these were the average ambient temperature, sky temperature and the wind speed. For a proper analysis two set of constants were chosen. The first set was average values for February and the second set was for July; the values of these can be seen in Table 1.

Table 3 Average weather data for two months in 2008 for Helsinki

	February 2008	July 2008
T_{amb} (℃)	0.73	17.62
T_{sky} (℃)	-7.51	3.67
$v\ (m/s)$	5.18	4.01

To determine the pressure range for the gas used to be analyzed by the model, calculations were made of the transmittance of a HPDE window at different pressures. These calculations were made by the use of Equation 31 and Equation 32 and resulted in Figure 6. For calculations of the window thickness, the modus of rupture (MR) is 16MPa (10). The transmittance of the 0.5mm-polyethylene film was used as a reference value for the transmittance calculations; the transmittance of the 0.5mm-polyethylene film was τ=0.44 (11). Figure 6 shows the result of these calculations and those only small overpressures can be used in the roof window system. Therefore, the range for the analysis of the model was chosen to be 1-1.115bar.

Copyright © 2010 by ASME

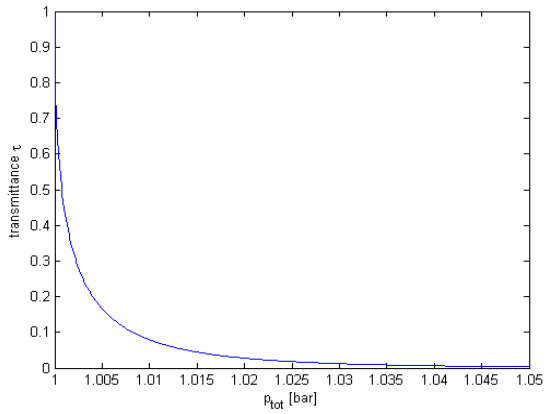

Figure 6 Transmittance of a HPDE window at increasing pressures

RESULTS AND DISCUSSION

By the use of the models presented in the section above, calculations were made as regards to the influence of the gas pressure and length of the gas enclosures on the heat transfer of the roof window system. Calculations for the insulation mode of the roof window with average values for February are presented in Figure 7. They show an increased heat flow at low pressures and at short gas path lengths (i.e. spacings between glass surfaces). The results are consistent with that expected as heat transfer by conduction and radiation is decreased with increasing gas lengths and thicker windows originating from higher pressures.

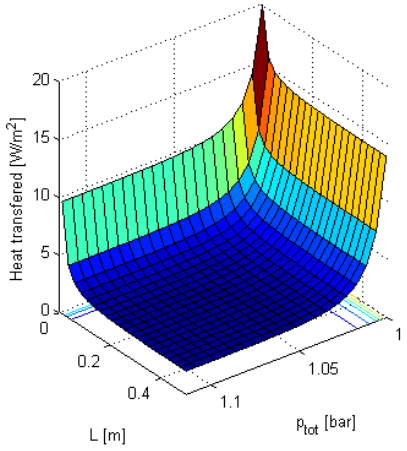

Figure 7 Total heat transfer for insulation mode in February

The difference between the cooling mode and the insulation mode is negligible (mW/m^2), as presented in Figure 8. The same calculations were also made with the average weather data for July. The results from these calculations are presented in Figure 9 and in Figure 10. The total heat flow presented in Figure 9 is larger than Figure 10 since colder ambient and sky temperatures are used in the calculations.

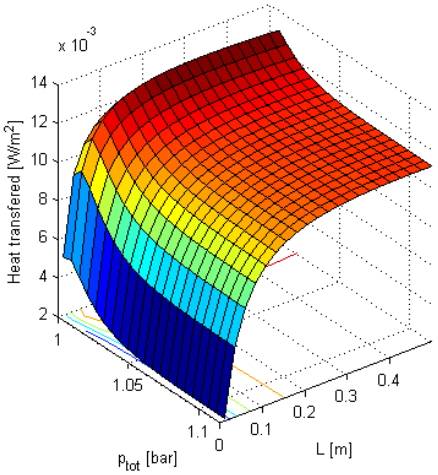

Figure 8 Difference in the total heat transferred in February

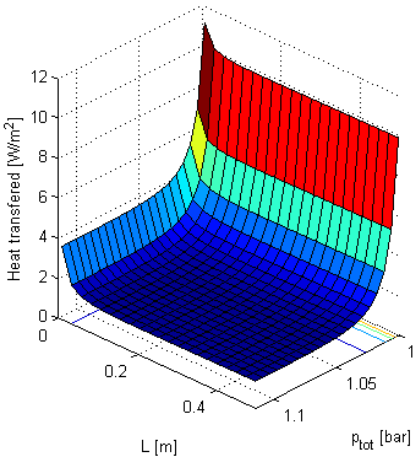

Figure 9 Total heat transfer for insulation mode in July

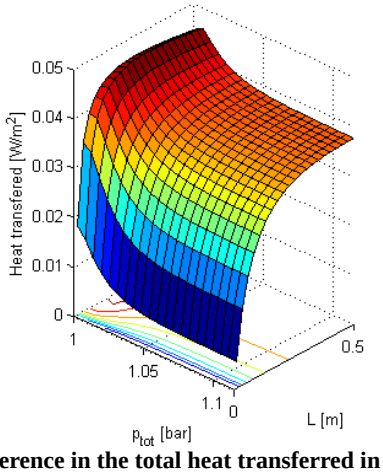

Figure 10 Difference in the total heat transferred in July

However, the model analysis done for both of the average values of February and of July, demonstrate no significant cooling by the cooling mode. Only minor cooling effects can be observed, these presented in Figure 8 and in Figure 10. This contradiction to the expected results originates from the selected method of calculation. This method fails to

Copyright © 2010 by ASME

calculate both the radiation part in combination with the convection and conduction part, it does not take into consideration that the gas in the enclosure emits more heat radiation when the two gas layers are connected; it only calculates the increased convective heat transfer of the system. The suitability of using the additive method has also been reported being unsuitable for calculations like these (5).

The model analysis shows, however, how the roof window system operates and therefore a set of parameters can be chosen for simulations. These parameters consist of the length of the gas enclosures and the total pressure of the gas. In the simulation, the gas pressure was chosen to be 1.005 bar and the lengths of the gas enclosures were set to 0.2m each.

Simulations of the roof window for February gave an average heat transfer of 4.93 W/m^2 and a total heat flow through the system for the whole month was calculated to be 12.3 MJ/ m^2. The result of the simulation can be seen in Figure 11, where the heat transfer is presented for the whole month.

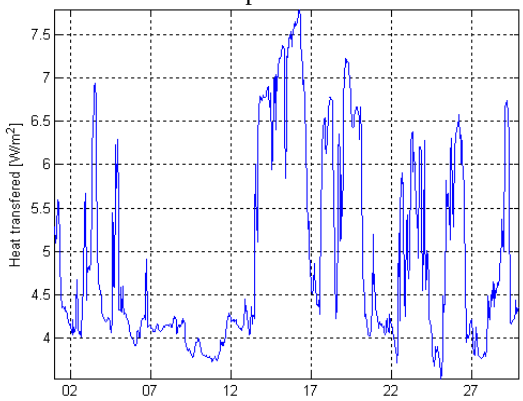

Figure 11 Heat transfer through the system during February

Simulations of the roof window for July gave an average heat transfer of 3.5276 W/m^2 and the total heat flow through the system was calculated to be 8.8 MJ/ m^2.

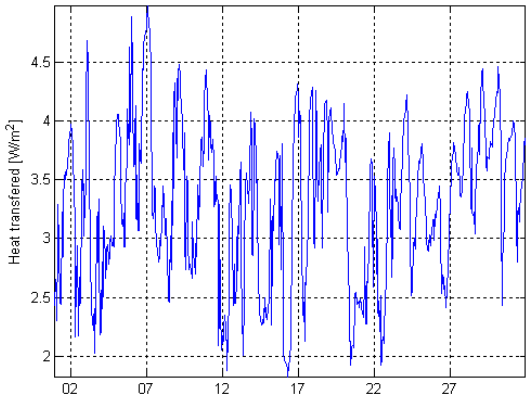

Figure 12 Heat transfer through the system during July

The simulations also reconfirm the results of the modeling that is that no extra cooling could be simulated with this model.

CONCLUSIONS

This article has presented an idea of using regulated roof windows for cooling purposes by radiative cooling. If this system were successfully implemented, savings could be reached by the avoided usage of conventional energy intensive cooling methods. However, more work has to be done and a different approach with a new model has to be made. That model should better combine the different heat transfer methods, and also take into account the wavelength dependence, in the heat radiation part, of the gas and of the plastic. The wavelength dependence was not taken into consideration in this model as the heat radiation part, was based on gray assumption.

ACKNOWLEDGMENTS

This work is funded by Maj and Tor Nessling Foundation projects 2009301 and 2010362 “Solar heat engineering and carbon dioxide: energy recovery using a greenhouse gas”, and the Foundation for Åbo Akademi University.

References

1. *Heat flow control and energy recovery using CO2 in double glass arrangements.* **Zevenhoven, Ron and Fält, Martin.** Phoenix : ES2010, 2010. ES2010-90189.

2. *Radiative cooling of buildings with flat-plate solar collectors.* **Erell, Evyatar and Etzion, Yair.** 35, s.l. : Building and Enviroment, 2000, pp. 297-305.

3. *The cooling performance of a radiator based roof component.* **Dimoudi, A and Androutsopoulos, A.** 80, s.l. : Solar Energy, 2006, pp. 1039-1047.

4. **Nilsson, Torbjörn and Niklasson, Gunnar.** Radiative cooling during the day: simulations and experiments on pigmented polyethylene cover foils. *Solar Energy Materials and Solar Cells.* 1995, 37, pp. 93-118.

5. **Modest, Michael F.** Radiation combined with conduction and convection. *Radiative Heat Transfer.* San Diego : Elsevire Science, 2003, pp. 680-727.

6. **Martienssen, W and Warlimont, H.** Glasses. *Springer Handbook of Condensed Matter and Materials Data.* s.l. : Springer Berlin Heidelberg, 2005, pp. 526-568.

7. **Parker, Danny S.** *Theoretical Evaluation of the NightCool Nocturnal radiation cooling concept.* Florida : Florida Solar Energy Center, 2005. p. 40. FSEC-CR-1502-05.

8. **Holman, Jack P.** Natural Convection Systems. *Heat Transfer.* S I metric Edition. Singapore : McGraw-Hill, 1989, pp. 323-358.

9. **Davies, Grenfell Morris.** Heat Transfer by Air movement. *Bulding Heat Transfer.* West Sussex : John Wiley & Sons Ltd, 2004, pp. 75-110.

10. **Youssef, H A, et al.** Studies of Sugrarcane Bagrasse Fiber Thermoplastics Composites. *Journal of Elastomers and Plastics.* 2009, 41, pp. 245-262.

11. **Tsilingris, P T.** Comparative evaluation of the infrered transmission of polymer films. *Energy Conversion & Management.* 2003, 44, pp. 2839-2856.

12. **Modest, Michael F.** Radiative properties of molecular gases. *Radiative Heat Transfer.* San Diego : Elsevier Science, 2003, pp. 288-356.

Copyright © 2010 by ASME

ANNEX A
CALCULATION OF GAS EMMISSIVITY

The gas that is used in this article is a gray gas that follows Equation 56.

$$\epsilon = \alpha = 1 - \tau \tag{56}$$

The emissivity of a gas or a gas mixture of CO_2 and H_2O can be calculated by using 57 62 (12).
First, the emissivity of a gas is calculated at one bar with Equation 57.

$$\epsilon_0\left(p_a L, p = 1\ bar, T_g\right) = exp\left[\sum_{i=0}^{M}\sum_{j=0}^{N} c_{ij}\left(\frac{T_g}{T_0}\right)^j \left(log_{10}\frac{p_a L}{(p_a L)_0}\right)^i\right], T_0 = 1000, (p_a L)_0 = 1\ bar\ cm \tag{57}$$

Then the result is corrected for different pressure conditions with Equation 58.

$$\frac{\epsilon\left(p_a L, p, T_g\right)}{\epsilon_0\left(p_a L, 1\ bar, T_g\right)} = 1 - \frac{(a-1)(1-P_E)}{a+b-1+P_E} exp\left(-c\left[log_{10}\frac{(p_a L)_m}{p_a L}\right]^2\right) \tag{58}$$

If the gas contains both CO_2 and H_2O a correction has to be made due to the overlap of the emissivity bands this is done by the use of Equations 59 and 60.

$$\Delta\epsilon = \left[\frac{\zeta}{10.7 - 101\zeta} - 0.0089\zeta^{10.4}\right]\left(log_{10}\frac{(p_{H_2O} + p_{CO_2})L}{(p_a L)_0}\right)^{2.76} \tag{59}$$

Where ζ is given by Equation 60.

$$\zeta = \frac{p_{H_2O}}{p_{H_2O} + p_{CO_2}} \tag{60}$$

The different emissivities are then obtained by Equation 61.

$$\epsilon_i\left(p_i L, p, T_g\right) = \epsilon_i\left(p_i L, 1\ bar, T_g\right)\left(\frac{\epsilon}{\epsilon_0}\right)\left(p_i L, p, T_g\right)_i \tag{61}$$

After which the total emissivity can be calculated by Equation 62.

$$\epsilon_{H_2O+CO_2} = \epsilon_{CO_2} + \epsilon_{H_2O} - \Delta\epsilon\left(p_{H_2O}L, p_{CO_2}L\right) \tag{62}$$

In Equation 57 to 62 the constants are given by Table 4 for calculation of the emissivity of the CO_2 and Table 5 for H_2O.

Table 4 The correlation constants needed for the calculation of the emissivity for CO_2

M, N	2,3
$\begin{bmatrix} c_{00} & \cdots & c_{N1} \\ \vdots & \ddots & \vdots \\ c_{0M} & \cdots & c_{NM} \end{bmatrix}$	$\begin{bmatrix} -3.9893 & 2.7669 & -2.1081 & 0.39163 \\ 1.2710 & -1.1090 & 1.0195 & -0.21897 \\ -0.23678 & 0.19731 & -0.19544 & 0.044644 \end{bmatrix}$
P_E	$(p + 0.28p_a)/p_0$
$(p_a L)_m/(p_a L)_0$	$\begin{cases} 0.054/t^2, & t < 0.7 \\ 0.225t^2, & t > 0.7 \end{cases}$
a	$1 + {0.1}/{t^{1.45}}$
b	0.23
c	1.47
$T_0 = 1000\ K, p_0 = 1\ bar, t = {T}/{T_0}, (p_a L)_0 = 1\ bar\ cm$	

Table 5 The correlation constants needed for the calculation of the emissivity for H_2O

M, N	2,2
$\begin{bmatrix} c_{00} & \cdots & c_{N1} \\ \vdots & \ddots & \vdots \\ c_{0M} & \cdots & c_{NM} \end{bmatrix}$	$\begin{bmatrix} -2.2118 & -1.1987 & 0.035596 \\ 0.85667 & 0.93048 & -0.14391 \\ -0.10838 & -0.17156 & 0.045915 \end{bmatrix}$

Copyright © 2010 by ASME

P_E	$(p + 2.56p_a/\sqrt{t})/p_0$
$(p_aL)_m/(p_aL)_0$	$13.2t^2$
a	$\begin{cases} 2.114, & t < 0.75 \\ 1.888 - 2.053log_{10}t, & t > 0.75 \end{cases}$
b	$1.10/t^{1.4}$
c	0.5
$T_0 = 1000\ K, p_0 = 1\ bar, t = T/T_0, (p_aL)_0 = 1\ bar\ cm$	

Copyright © 2010 by ASME